Protist, Vol. 167, 82–92, February 2016
http://www.elsevier.de/protis
Published online date 19 November 2015

Protist

ORIGINAL PAPER

Towards a Better Understanding of the Life Cycle of *Trypanosoma copemani*

Adriana Botero[a,1], Peta L. Clode[b], Christopher Peacock[c,d], and R.C. Andrew Thompson[a]

[a]School of Veterinary and Life Sciences, Murdoch University, South Street, Murdoch, WA 6150, Australia
[b]Centre for Microscopy, Characterisation and Analysis, University of Western Australia, Stirling Hwy, Crawley, WA 6009, Australia
[c]School of Pathology and Laboratory Medicine, University of Western Australia, Crawley, WA 6009, Australia
[d]Telethon Kids Institute, 100 Roberts Road, Subiaco, WA 6008, Australia

Submitted June 30, 2015; Accepted November 11, 2015
Monitoring Editor: Dmitri Maslov

Trypanosoma copemani **has been found infecting several threatened/endangered marsupial species within Australia and is thought to be a key player in the rapid decline of the woylie (*Bettongia penicillata*). To better understand the biology and life cycle of this parasite, the growth requirements, and kinetics of infection of two newly described genotypes, *T. copemani* G1 and G2, were investigated and compared with the *T. cruzi* strain-10R26 *in vitro.* Both G1 and G2 were able to infect all four cell lines tested. The number of infected cells where at least one intracellular amastigote of *T. copemani* G1 and G2 was seen was below 7% and 15% respectively in most cell lines. However, in *VERO* cells the rate of infection for *T. copemani* G2 was 70%-approximately seven and two times higher than for G1 and *T. cruzi* respectively. Despite the higher infection rate, the number of intracellular forms of *T. copemani* G2 was lower compared with *T. cruzi*, and intracellular replicating forms were not observed. The capability of *T. copemani* G2 to infect cells may have important consequences for pathogenicity and suggests it might employ similar strategies to complete its life cycle in the vertebrate host to those seen in *T. cruzi*.**

Key words: *Trypanosoma copemani*; *T. cruzi*; acidocalcisomes; cell infection; pathogenicity; social motility.

Introduction

Trypanosoma comprises a large number of species and subspecies with complex life cycles that involve both invertebrate and vertebrate hosts. The life cycle in the vertebrate host varies from one species to another and may involve different stages of the parasite. This variability at least in part lies in the ability of some trypanosomes to replicate inside host cells. The replication of trypanosomes such as *T. theileri*, a parasite of cattle, *T. lewisi* a parasite of rodents, fish and birds trypanosomes, and trypanosomes from the *T. brucei* complex that infect humans and several ungulates, occurs extracellularly in peripheral blood where they replicate as trypomastigotes. This stage of the parasite has also been found in extravascular sites of lymph nodes, kidney, spleen, bone marrow, and brain (D'Alessandro and Behr 1991; Hoare 1972; Molyneux 1976; Rodrigues et al. 2003; Sudarto et al. 1990; Tizard et al. 1980). In contrast,

[1]Corresponding author; fax +61 8 93602466
e-mail L.BoteroGomez@murdoch.edu.au (A. Botero).

http://dx.doi.org/10.1016/j.protis.2015.11.002

T. cruzi, the agent of Chagas disease in humans does not replicate in blood, but presents a life cycle that involves invasion and replication inside host cells (De Souza et al. 2010; Oliveira et al. 2009). During its life cycle in the vertebrate host, *T. cruzi* alternates between two different developmental stages, the bloodstream trypomastigote (non-dividing form) and the amastigote in tissues (intracellular and replicative form). Bloodstream trypomastigotes invade a large number of mammalian cells, and once in the cytoplasm of the cell they differentiate into amastigotes. After an intense multiplicative phase, amastigotes transform into trypomastigotes that are released upon rupture of the cells. Trypomastigotes infect neighbouring cells and are eventually disseminated throughout the body, leading to the establishment of the infection in several tissues in the host (De Souza et al. 2010). A few other *Trypanosoma* species phylogenetically related to *T. cruzi* are capable of infecting and multiplying within cells. For example, *T. dionisii* and *T. erneyi*, both trypanosomes of bats, are capable of invading and replicating inside cells and have been shown to exhibit some similar features of host cell invasion to *T. cruzi* (Lima et al. 2012, 2013; Oliveira et al. 2009). For *T. rangeli*, a parasite that infects a large number of mammals in Central and South America, contradictory results have been reported regarding the life cycle within the vertebrate host. The replication of this species does not occur in blood, however, its ability to infect and replicate inside cells is controversial, with some studies supporting cell invasion and others not (Eger-Mangrich et al. 2001; Tanoura et al. 1999; Zúñiga et al. 1997a,b).

Within Australia, several species and genotypes of trypanosomes have been described infecting wildlife. To date, only a few trypanosomes have been isolated in culture from Australian marsupials, namely *T.* sp. H25, *T.* sp. H26, and *T. copemani* (Austen et al. 2009; Noyes et al. 1999). However, the description of these species has been largely based on molecular data, host occurrence, and/or morphology of blood forms, and little is known about the distinct morphological and functional forms of these parasites during their life cycle in the vertebrate host or under experimental conditions in axenic media. More recently, based on 18S rDNA and g*GAPDH* sequences, two new different genotypes within the *T. copemani* clade (*T. copemani* G1 and G2) were detected infecting different marsupials (Botero et al. 2013). Interestingly, *T. copemani* G2 was found in several tissues and blood, while *T. copemani* G1 was only found in blood, suggesting marked differences in their biological behaviour. Although, 18S rDNA and g*GAPDH* phylogenies showed that *T. copemani* does not belong to the *T. cruzi* clade all members of which being capable of intracellular replication, in vitro experiments showed that both *T. copemani* G1 and G2 were capable of infecting cells (Botero et al. 2013). Differences in infection rates, intracellular replication, and media requirements for growth have not been evaluated.

Considering the biological differences previously observed between both strains of *T. copemani*, the aims of this study were to (i) determine and compare their optimal growth requirements and different morphological and functional forms in vitro; and (ii) evaluate and compare their kinetics of infection in four different cell lines, using the intracellular *T. cruzi* as a positive control of infection and as an indication of pathogenicity.

Results

Trypanosome Growth Curves

Minor differences in growth requirements between *T. copemani* G1 and G2 were observed. Both strains showed a growth rate significantly higher in RPMI 1640, followed by Grace's and HMI-9 media. However, Grace's and HMI-9 media supported the growth of *T. copemani* G1 better than G2. Trypanosomes growing in RPMI 1640 were seen actively dividing until day 8 post-inoculation. At this time they reached the maximum number, before beginning to die due to nutrients in the medium being exhausted (data not shown). The doubling growth time of parasites in RPMI 1640 and Grace's media was approximately 2 days. Growth curves of both *Trypanosoma* strains grown separately in the three different media are shown in Figure 1. Schneiders medium failed to support the growth of either strain of *T. copemani*.

Role of Haemin in Growth

T. copemani G1 and G2 were grown in different concentrations of haemin between 2.5 mg/l to 20 mg/l. Although, both strains of *T. copemani* grew well without haemin, depending on concentration, the addition of haemin to the media significantly improved growth, mobility, and motility. Growth curves could not be generated due to trypanosomes being compacted firmly in nests or rosettes that could not be homogeneously separated. Therefore, trypanosome growth was followed as a qualitative observation of proliferation (size of nests), mobility (ability to move spontaneously

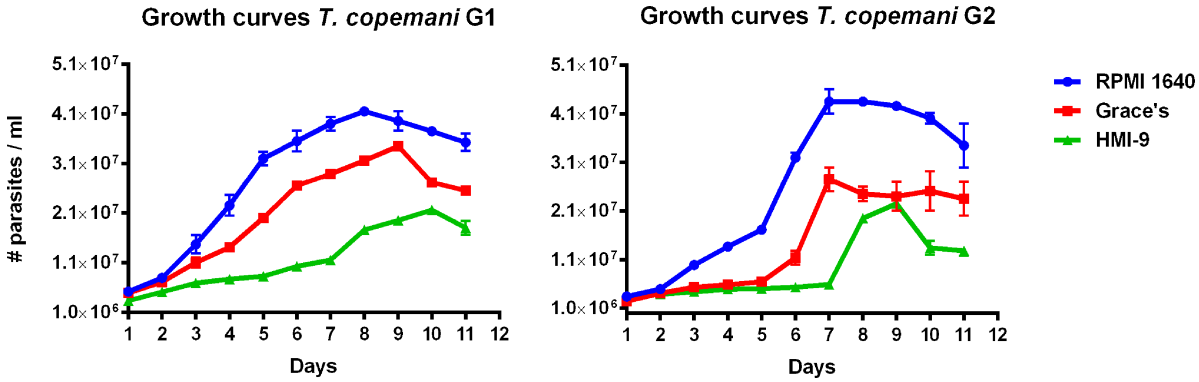

Figure 1. Growth curves of *Trypanosoma copemani* strains in different media, **A**: *Trypanosoma copemani* G1; **B**: *Trypanosoma copemani* G2. These data represent the mean of three independent experiments (triplicate values in each experiment) ± SEM.

and actively - does not involve displacement), and motility (ability to move spontaneously and actively - involves displacement) under the microscope. The haemin concentrations that produced more and larger nests were 2.5 mg/l and 10 mg/l for *T. copemani* G1 and G2, respectively. These concentrations improved trypanosome activity in the media in terms of mobility and motility, and free trypanosomes (not in the process of division in nests) moved continuously from side to side in the wells in both *T. copemani* G1 and G2 cultures. However, at the other concentrations of haemin (5 mg/l, 15 mg/l and 20 mg/l) trypanosomes were not very active and did not divide quickly. Interestingly, trypanosomes formed groups of big and small densely-packed cells (nests) within 24 h post-plating. Nests moved across the plate surface, recruiting neighboring nests and forming fusions of large groups as shown in the sequential images (Supplementary Material Fig. S1). Haemin concentrations higher than 10 mg/l and 15 mg/l decreased the growth rate of both *T. copemani* G1 and G2 respectively and also induced morphological changes. At these haemin concentrations most of the parasites adopted a spherical shape and partially or completely lost the prominent flagellum resembling the amastigote and spheromastigote forms.

Morphology

Peripheral blood smears from woylies (*Bettongia penicillata*) infected with *T. copemani* G1 and G2 showed blood trypomastigotes with large body width and length. These forms exhibited a small rounded kinetoplast and a larger, oval nucleus. The kinetoplast stains densely purple and is positioned close to the nucleus in the posterior end of the cell. The nucleus stains light pink and is located in the centre of the cell. Blood trypomastigotes presented also a conspicuous undulating membrane with well-pronounced undulations and flagella, which originate just anterior to the kinetoplast (Fig. 2A). Gross morphological features were very similar between *T. copemani* G1 and G2 with non-significant differences in body width (width: 6.0 ± 0.1 *T. copemani* G1, 6.5 ± 0.1 *T. copemani* G2) (μm ± SEM), but statistically significant differences in body length (Fisher exact test, $P = 0.001$) were found (length: 35.8 ± 0.5 μm *T. copemani* G1, 39.9 ± 0.2 μm *T. copemani* G2) (μm ± SEM). Dividing forms were never observed in blood smears.

In the exponential or logarithmic phase of trypanosome growth in culture, the epimastigote was the predominant form. Epimastigotes presented highly variable shapes with a small kinetoplast positioned adjacent to the nucleus. Some of the forms were long and thin undergoing binary division, giving rise to nests or rosettes and transitional forms of variable shape and body (Fig. 2B). Some of these transitional forms were spheromastigotes (Fig. 3A) that were often seen to be dividing and trypomastigotes with an undulating membrane (Fig. 3B).

Both strains reached the stationary or non-proliferative phase when the concentration of parasites was approximately $4x10^7$ parasites/ml (Fig. 1). Most parasites at this late phase were slender, long flagellates that exhibited a less prominent undulating membrane and a rounded, small kinetoplast. This was positioned far away from an elongated nucleus and close to the posterior end of the cell resembling metacyclic trypomastigote forms (Figs 2C and 3B).

T. copemani G1 and G2 share common morphological features with other trypanosomatids. Trypomastigotes, epimastigotes, and

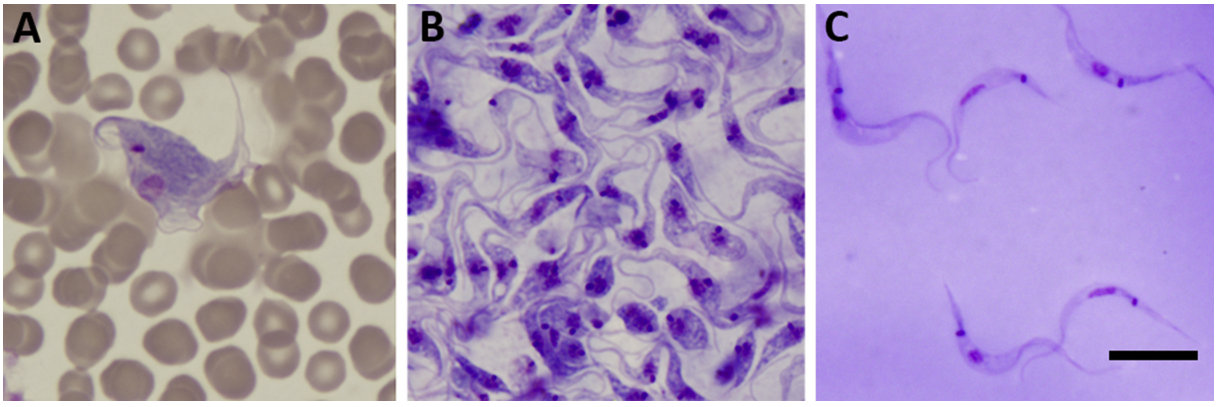

Figure 2. Light micrographs of Diff-quick stained *Trypanosoma copemani* G2. **A**: trypomastigote form in a blood smear from a woylie; **B**: epimastigote forms growing in culture; **C**: stationary phase culture forms. Scale bar: 10 μm.

spheromastigotes possess numerous spherical electron-dense particles throughout the cytoplasm, which appear morphologically similar to acidocalcisomes described in other trypanosomatids (Lima et al. 2012; Miranda et al. 2000). The size and number of acidocalcisomes per cell was variable ranging from only 3 or 4 large acidocalcisomes to more than 10 small acidocalcisomes (Fig. 4). These structures were also observed in live cells (Fig. 5). A dense corset of cross-linked microtubules that form the subpellicular membrane was observed surrounding the body of the cell (Fig. 4A). Scanning electron micrographs showed flagella that emerged from a small invagination in the cell body, the flagellar pocket (Fig. 6). The flagellum of both strains of *T. copemani* consisted of an axoneme with nine duplets of microtubules in the periphery with two microtubules at the center and a paraflagellar rod (Fig. 6, box).

Kinetics of Infection

Both strains of *T. copemani* were able to infect all cell lines used. However, significant differences in the infection rate were seen between *T. copemani* G1 and G2, and between *T. copemani* G1/G2 and *T. cruzi* in all cell lines (Fisher exact test, $P < 0.0001$). Trypomastigotes of both strains of *T. copemani* were commonly observed attached to cells (Fig. 7). They appeared to attach to the cell by the posterior end in a manner similar to *T. cruzi*. Scanning electron microscopy further confirmed that some attached trypanosomes were invading cells and commonly revealed debris of dead cells surrounded by amastigotes and trypomastigotes after the second day of infection (Fig. 8). However, no sign of infection was seen when these cell-free trypomastigotes from second day infected cells were used to infect new cells. Intracellular

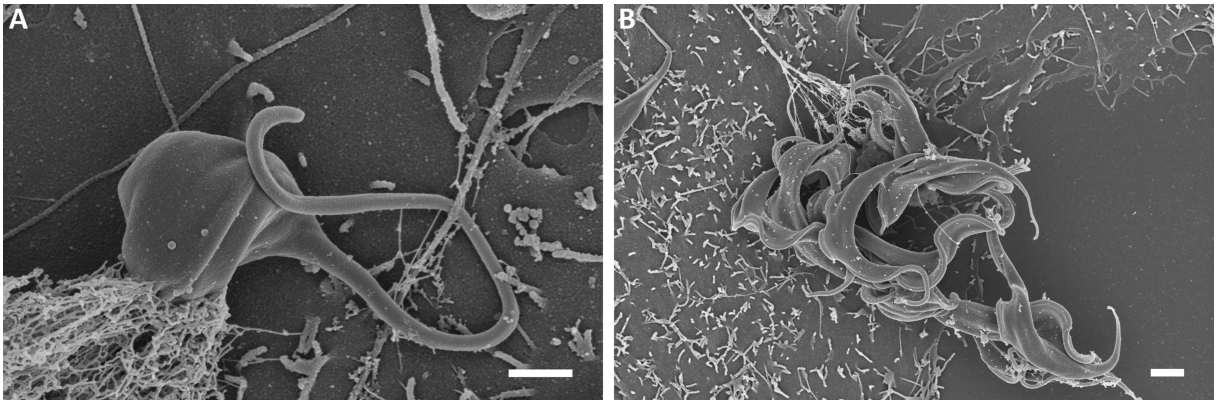

Figure 3. Scanning electron micrographs of *Trypanosoma copemani* G2 grown in culture at 28 °C and 37 °C with *VERO* cells. **A**: spheromastigote at 28 °C; **B**: trypomastigotes at 37 °C. Scale bars: 1 μm (A) and 2 μm (B).

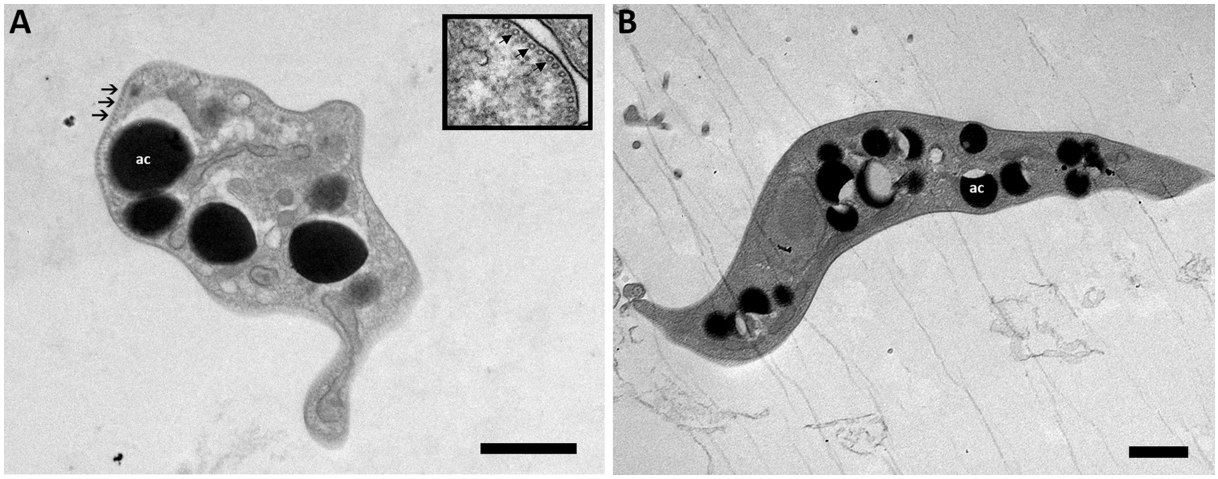

Figure 4. Transmission electron micrographs showing acidocalcisomes in various growth forms of *Trypanosoma copemani* G2. **A**: epimastigote; **B**: trypomastigote. Acidocalcisomes (ac); subpellicular microtubules (cytoskeleton, arrows). Scale bars: 1 μm (A), and 0.5 μm (B).

T. copemani G2 amastigotes containing acidocalcisomes were routinely identified within the host cell cytoplasm. However, no intracellular replication was observed in the cytoplasm of any cell line infected with either *T. copemani* G1 or G2. Figure 9 shows a representative image from several acquired images of an intracellular amastigote of *T. copemani* G2.

Intracellular amastigotes of *T. copemani* G1 and G2 and *T. cruzi* were first observed at 6 hours post-infection in *L6* cells. The progression of the infection was similar for *T. copemani* G1 and G2. However, the number of cells infected with *T. copemani* G2 was significantly higher (Fisher exact test, $P < 0.0001$). The highest rate of infection by *T. copemani* G1 was 5% at 48 hours post-infection, while the highest rate of infection by *T. copemani* G2 was 15% at the same time post-infection. In contrast, the percentage of *L6* cells infected with *T. cruzi* was significantly higher (Fisher exact test, $P < 0.0001$), increasing rapidly after 24 hours post-infection and reaching a peak of 82% at 72 hours post-infection (Fig. 10A). Cells infected with *T. cruzi* exhibited a larger number of intracellular amastigotes at 12, 24, 48, 72 and 96 hours post-infection compared with both *T. copemani* G1 and G2, where no more than three amastigotes were seen inside cells at any time post-infection (Fig. 10A). After 48 hours post-infection, *T. cruzi*

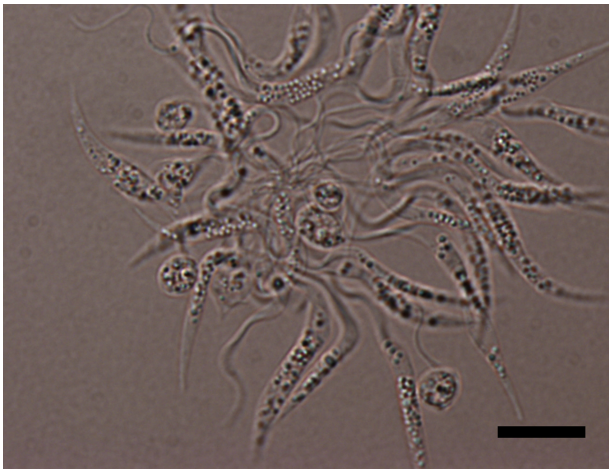

Figure 5. Light micrograph showing numerous acidocalcisomes (light green dots) within the cytoplasm of *Trypanosoma copemani* G2. Scale bar: 10 μm.

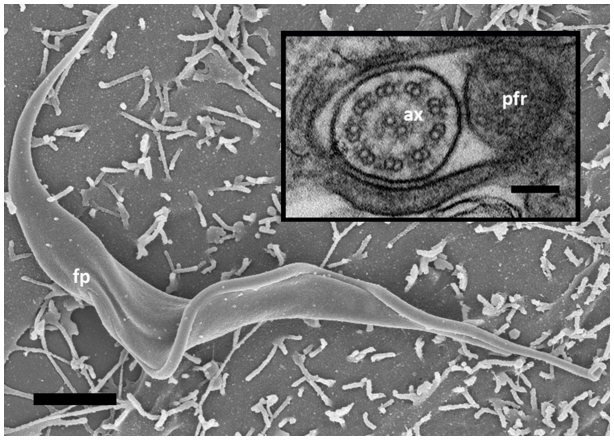

Figure 6. *Trypanosoma copemani* G2 trypomastigote and the flagellum structure. Flagellar pocket (fp); axoneme (ax); paraflagellar rod (pfr). Scale bar: 2 μm (inside box 0.1 μm).

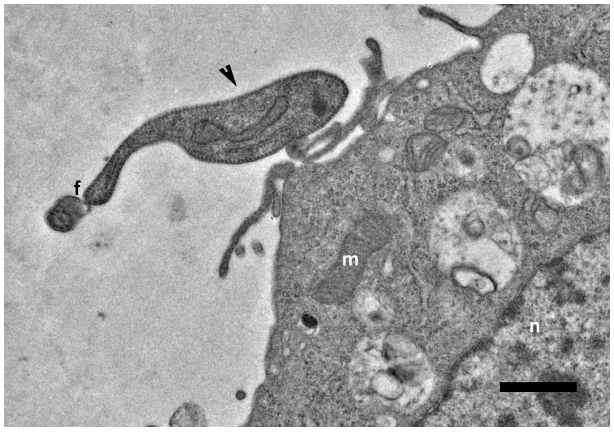

Figure 7. Transmission electron micrograph of a trypomastigote (arrow) of *Trypanosoma copemani* G2 attached to a *VERO* cell. Flagellum (f); *VERO* cell mitochondria (m); *VERO* cell nucleus (n). Scale bar: 1 μm.

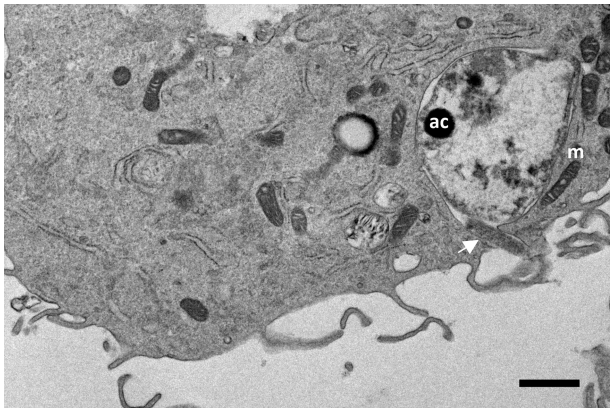

Figure 9. Transmission electron micrograph of an intracellular amastigote of *Trypanosoma copemani* G2 in *VERO* cells. Remaining short flagellum (arrow); Amastigote acidocalcisome (ac); *VERO* cell mitochondria (m). Scale bar: 1 μm.

amastigotes were seen differentiating into trypomastigotes inside cells (Supplementary Material Fig. S2).

Both *T. copemani* G1 and G2, and *T. cruzi* were able to infect *VERO* cells at 6 hours post-infection, with no significant differences in the number of cells infected (Fisher exact test, $P < 0.07$). An increase in the number of cells infected was observed over the time, reaching a maximum of 7% with *T. copemani* G1, 70% with *T. copemani* G2, and 33% with *T. cruzi* at 48 hours post-infection. After this time, the percentage of infected cells decreased for all trypanosomes (Fig. 10B). *T. copemani* G2 induced a significantly stronger infection at all times post-infection when compared with *T. cruzi* (Fisher exact test, $P < 0.0001$). Although almost 70% of cells were infected with *T. copemani* G2 and only 33% of cells were infected with *T. cruzi* at 48 hours post-infection, the number of intracellular amastigotes was higher in *T. cruzi* infected cells (Fig. 10B).

In both human-derived cell lines *HCT8* and *THP1*, the rate of infection of *T. copemani* G1 and G2 was very similar (Fig. 10C). Neither *T. copemani* G1 or G2 were able to infect more than 7% of either cell line at any time post-infection. In contrast, the percentage of cells infected with *T. cruzi* was significantly higher (Fisher exact test, $P < 0.0001$), and showed a continual increase in infection rates, which peaked at 34% in *HCT8* cells and 40% in *THP1* cells at 96 hours post-infection. Active intracellular replication was clearly evident only in

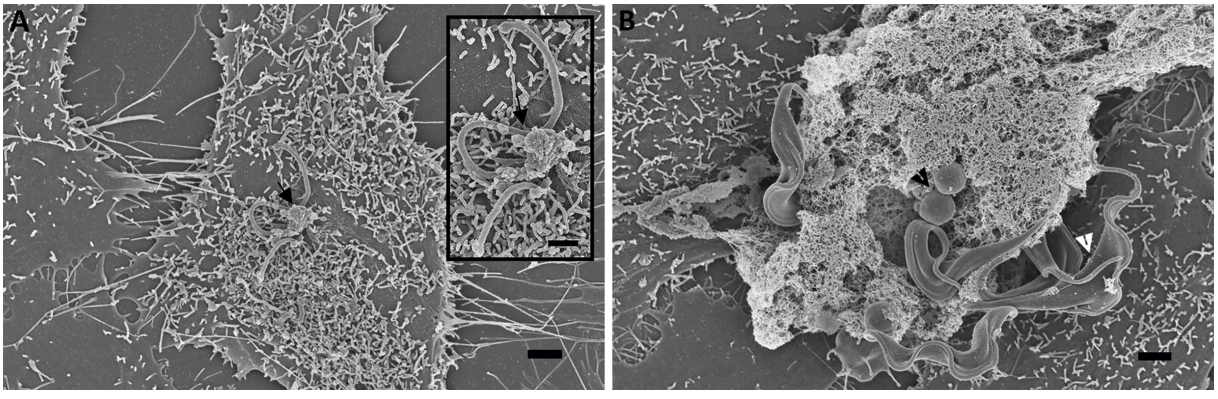

Figure 8. Scanning electron micrographs of trypomastigotes and amastigotes of *Trypanosoma copemani* G2 in *VERO* cells. **A**: trypomastigote invading a cell (flagellum: black arrows); **B**: trypomastigotes (withe head arrow) and amastigotes (black head arrow) with cellular debris. This image has been used and adapted with permission from Botero et al. 2013. Scale bars: 1 μm (A) (inside box 1 μm) and 2 μm (B).

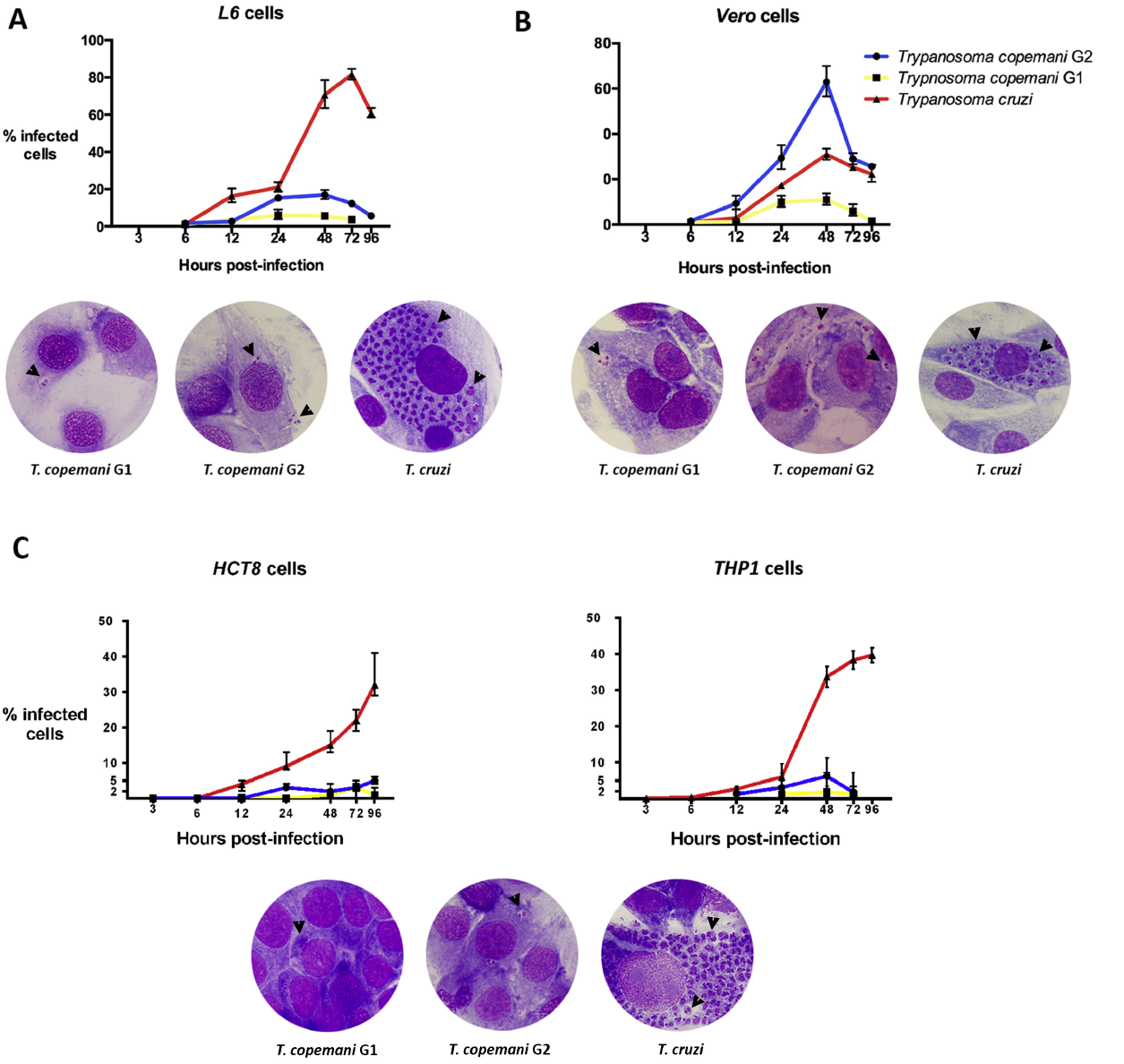

Figure 10. Kinetics of infection and intracellular development of *Trypanosoma copemani* G1 and G2, and *Trypanosoma cruzi*. **A**: *L6* cells; **B**: *VERO* cells. **C**: *HCT8* and *THP1* cells. Diff-Quick stained images at the base of each graph represent cells infected and show intracellular amastigotes (arrows). Unfortunately, good quality images of *THP1* cells could not be obtained. These data represent the mean of three independent experiments (triplicate values in each experiment) ± SEM.

T. cruzi where large numbers of amastigotes were seen inside cells (Fig. 10C).

Discussion

A few species of *Trypanosoma* have been isolated in culture from Australian mammals (Austen et al. 2009; Noyes et al. 1999). However, the life cycle of these parasites in the vertebrate host remains unknown. To date, the only in vitro study investigating the life cycle of Australian trypanosomes showed that two *Trypanosoma* isolates, *T.* sp. H25 and *T.* sp. H26, isolated from a kangaroo and a wombat respectively, failed to infect *LLCMK2* cells (Rhesus monkey kidney cells) in vitro (Noyes et al. 1999), while a more recent study (Botero et al. 2013) demonstrated that *T. copemani* is able to invade cells *in vitro*. Furthermore, the finding of *T. copemani* DNA in tissues and structures in the

cytoplasm of these tissue cells consistent with amastigote forms of other *Trypanosoma* species (Botero et al. 2013; Carreira et al. 1996), suggested a *T. copemani* life cycle in the marsupial host that involves migration to tissues, cell infection, and intracellular replication. This latest study (Botero et al. 2013) also showed that only *T. copemani* G2 was present in multiple marsupial host tissues, while *T. copemani* G1 was only found in blood. These results are complemented by the present study, which found marked differences in the rate of cell infection between both strains of *T. copemani*. Irrespective of the cell line used, *T. copemani* G1 infection rates were very low, always below 7% whereas *T. copemani* G2 was highly infective to *VERO* cells, with 70% of cells infected at 48 hours post-infection. We also found slight differences in size of both *T. copemani* G1 and G2 consistent with the previously described phenotypes 1 and 2 of *T. copemani* (Thompson et al. 2013). It seems that the life cycle of both *T. copemani* G1 and G2 are different, therefore raising the question as to whether they are two genotypes or actually different species. The fact that *T. copemani* G2 was highly infective to one cell line highlights the capacity of this parasite to infect cells in the marsupial host and raises questions about the potential virulence and pathogenicity of this parasite and its role in the rapid and substantial decline of the brush tailed bettong, or woylie (*Bettongia penicillata*) (Botero et al. 2013; Wayne et al. 2013a, b).

The *T. cruzi* 10R26 strain as well as *T. copemani* G2 exhibited significant differences in infectivity among cell lines. *T. copemani* G2's rate of infection in *VERO* cells was double the rate of infection produced by *T. cruzi*, while in *L6* and in both human-derived cell lines, *T. cruzi* showed a higher level of cell invasion. Interestingly, results that showed that the kidney of naturally infected marsupials are frequently infected with *T. copemani* G2 (Botero et al. 2013) are consistent with results described here in vitro, in which the kidney epithelial-derived *VERO* cell line was frequently invaded by *T. copemani* G2. However, no sign of active *Trypanosoma* multiplication was seen inside *VERO* cells. This apparent lack of intracellular replication of *T. copemani* G2 might be due to the origin of the cell line. It has been shown that the host genetic background plays an important role in susceptibility or resistance to infections with *T. cruzi* (Andrade et al. 2002). Therefore, the origin of the cell line could determine the success or failure of *in vitro* infections. The use of a better *in vitro* model, ideally a primary marsupial tissue derived cell line, or an inmortalised marsupial cell line, may support the intracellular replication of *T. copemani*. However, the finding of numerous amastigotes of *T. copemani* G2 in cells in tissues of naturally infected woylies (Botero et al. 2013) suggests that the parasite can invade and replicate. Additionally, the fact that dividing forms of this parasite have never been observed in the peripheral blood of marsupials suggests that division may be confined to tissues (Botero et al. 2013; Thompson et al. 2013). The similarity in the biological behaviour of *T. copemani* and *T. cruzi* suggests that these parasites might use similar strategies to complete their life cycle in the vertebrate host. Therefore, we have proposed a life cycle of *T. copemani* G2 in the vertebrate host that involves tissue migration, and cell infection (Fig. 11).

A nutritional requirement of all different species of *Trypanosoma* is that in vitro they need a haem-compound as a growth factor. Studies have shown that haemin plays an important role in growth and differentiation of trypanosomes (Lara et al. 2007). Although haemin was not necessary for the growth of *T. copemani* in vitro, it enhanced cell proliferation considerably. A haemin concentration of 2.5 mg/l added to Grace's medium was the optimum concentration for the growth of both strains of *T. copemani* in culture. Haemin concentrations higher than 15 mg/l produced markedly significant morphological changes. Most of the forms present in these cultures were spherical with a short or absent flagellum consistent with amastigote forms of other *Trypanosoma* species, suggesting that transformation from epimastigotes to amastigotes could be induced by high concentrations of haemin.

An interesting behaviour observed by both strains of *T. copemani* in culture was the movement of nests across the plate surface. Nests were observed recruiting neighboring smaller nests establishing large communities of cells similar to what has been described in bacteria in response to external signals (Harshey 2003) and what is termed "social motility" or SoMo (Velicer et al. 2000). *T. brucei* is also able to assemble into multicellular communities with polarised and coordinated movements that are not apparent in single cells and are in response to an external stimulus (Oberholzer et al. 2010). It has been suggested that SoMo in *T. brucei* may facilitate colonisation of host tissues, transmission, and may have an impact on pathogenesis (Bastin and Rotureau 2015; Imhof et al. 2014). The apparent SoMo observed in *T. copemani* could have some important consequences in infectivity and pathogenicity and might enhance their ability to colonise, penetrate, and migrate through different tissues in vertebrate and invertebrate hosts.

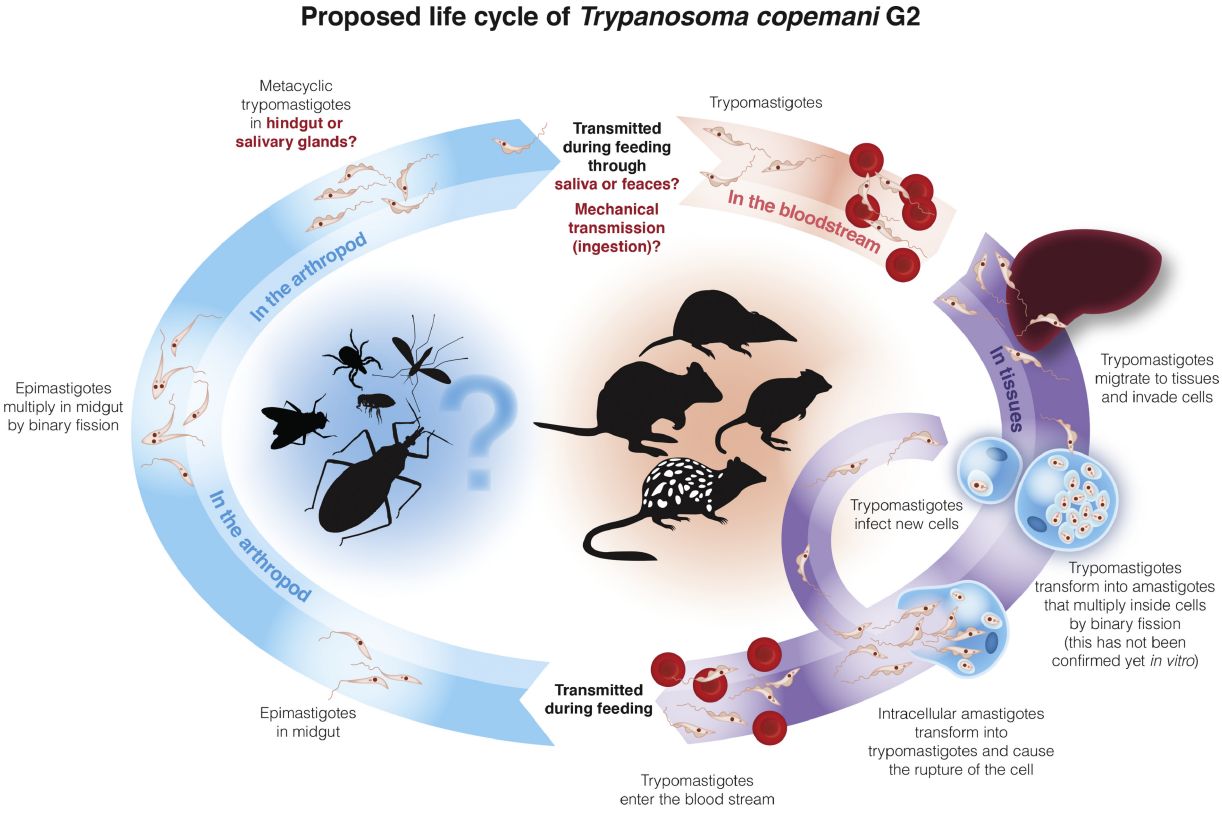

Figure 11. Proposed life cycle of *Trypanosoma copemani* G2 in the vertebrate host.

Conclusions

This study adds to the small number of trypanosomes that are known to be intracellular in mammalian hosts and reinforces previous findings of *T. copemani* G2 in several tissues of threatened and endangered Australian marsupials. Here, we have proposed a life cycle of *T. copemani* G2 in the vertebrate host that involves tissue migration and cell infection.

Methods

Trypanosome development in culture and growth curves: *T. copemani* G1 and G2 previously isolated from the blood of woylies (Botero et al. 2013) were grown at 28 °C in four different liquid media, RPMI 1640 (Roswell Park Memorial Institute 1640), HMI-9 (Iscove's modified DMEM-based), Schneider's (Schneider 1964) and Grace's (Grace and Brozostowski 1966) (Supplementary Material Table S1), and their growth and morphological changes in culture were examined. Trypanosome growth curves were generated. For this, $1x10^3$, $1x10^4$ and $1x10^6$ parasites were seeded in triplicate wells in a 96 well plate. The number of trypanosomes in each well was calculated using a haemocytometer chamber for eight consecutive days and growth curves were generated using the Prism 6 software (GraphPad Software, San Diego, California, USA). Trypanosomes were also growth at 28 °C and 5% CO_2 with VERO cells as a feeder layer to observe if it enhances growth and/or any change in morphology.

Evaluation of different concentrations of haemin on growth: Because haem-compounds play an essential role in trypanosome growth, the effect of haemin on growth and differentiation was investigated. Different concentrations of haemin, 2.5 mg/l, 5 mg/l, 10 mg/l, 15 mg/l and 20 mg/l were added to Grace's and RPMI 1640 media, as these media resulted in the best rate of growth. $1x10^6$ parasites were seeded into 24-well plates containing each medium with differing haemin concentrations, and trypanosome growth rate was determined by counting parasites in a haemocytometer chamber every day for six consecutive days.

Kinetics of infection: The non-phagocytic cell lines *L6* (rat skeletal myoblast cells), *VERO* (African green monkey kidney epithelial cells), and *HCT8* (human ileocecal adenocarcinoma cells) and a phagocytic cell line (macrophage-like cells) derived from the human monocyte cell line *THP1* were used. Cells were grown in RPMI medium supplemented with 10% foetal calf serum (FCS) at 37 °C and 5% CO_2. *THP1* cells were grown in media that also included phorbol 12-myristate 13-acetate (PMA). Monolayers of each cell line were trypsinised and seeded onto tissue culture-slides (16-wells) at a concentration of 1.5×10^3 cells/ml, and 24 hours later were infected with cultures from the stationary phase containing metacyclic trypomastigote forms of *T. copemani* G1 and G2 and *T. cruzi* 10R26 strain (TcIIa). For the infection of cells, the media in each well was discarded to remove non-adherent cells and then each well was infected with 100 µl of trypanosome suspension containing 1.5×10^5 trypanosomes/ml (1:10 cell/parasite ratio) of each strain. Slides were incubated at 37 °C and 5% CO_2. The progress of cellular infection was monitored at 3, 6,

12, 24, 48, 72, and 96 hours post-infection. Non-adherent parasites were removed by washing the culture-slides three times with phosphate buffer solution (PBS) at each interval of time. The supernatant from cultures at 48 hours post-infection containing trypomastigotes was added to new cells to investigate if they were able to infect new cells. Two days later, non-adherent parasites were removed as mentioned above. Coverslips were removed and culture-slides were air-dried and stained with the commercial Romanowsky-type stain 'Diff-Quik' for examination by light microscopy. The percentage of infected cells was determined under 100x magnification by counting 100 cells/well per triplicate using an optical microscope and comparing the number of cells containing intracellular parasites to the total number of cells. Infection Kinetic curves were generated using the Prism 6 software (GraphPad Software, San Diego, California, USA). Experiments were replicated on three separate occasions, and all cell lines and trypanosomes were stored in a liquid nitrogen cryobank at Murdoch University. *T. cruzi* 10R26 strain was kindly provided by Professor Michael A. Miles. This strain was originally isolated and prepared by the research group of Michel Tibayrenc at the Institut pour Recherce et Developpement in Montpellier, France.

Light, scanning and transmission electron microscopy: The morphology of trypanosomes from direct thin blood smears collected previously from woylies (Botero et al. 2013) and smears of logarithmic and stationary phase cultures were compared. Smears were fixed in methanol and stained with the commercial Diff-Quick staining system for examination by light microscopy. For scanning electron microscopy (SEM), culture forms were fixed in a 1:1 mixture of 5% glutaraldehyde in 0.01 M PBS: cell culture medium (pH 7.2), before being mounted on poly-L-lysine coated coverslips, progressively dehydrated through a series of ethanol solutions and critical point dried as previously described (Edwards et al. 2011). Coverslips were mounted on stubs with adhesive carbon, coated with 2 nm platinum (Pt) and imaged at 3 kV using the in-lens secondary electron detector on a Zeiss 55VP field emission SEM. For transmission electron microscopy (TEM), trypanosomes were also fixed in a 1:1 mixture of 5% glutaraldehyde in 0.01 M PBS: cell culture medium (pH 7.2). All subsequent processing was performed in a PELCO Biowave microwave, where samples were post-fixed in 1% OsO_4 in PBS followed by progressive dehydration in ethanol/acetone, before being infiltrated and embedded in the epoxy resin. Sections 120 nm-thick were cut with a diamond knife and mounted on copper grids. Digital images were collected from unstained sections at 120 kV on a JEOL 2100 TEM fitted with a Gatan ORIUS1000 camera.

For SEM of infection experiments, cells were pre-seeded on poly-L-lysine coated coverslips in 24-well plates (2 x 10^5 cells/well) and infected with *T. copemani* G1 and G2 as above. After 48 hours post-infection, the coverslips were removed, washed in PBS, fixed, and processed for SEM as described above. Similarly, for TEM, infected cells were trypsinised at 48 hours post-infection, fixed, processed and imaged as described above. Measurements of morphological features (length and width) were made using ImageJ v. 1.29x (National Institutes of Health, USA). All images shown are representative of several light, scanning and transmission electron microscopy images acquired in three independent experiments.

Statistical analyses: Statistical analyses were performed using GraphPad Prism 6 (GraphPad Software, San Diego, California, USA). Analysis of the data was performed using one-way and two-way analysis of variance (ANOVA). The results are expressed as means ± SEM (standard error of the mean).

Differences in the infection rate were assessed by using Fisher's exact test.

Competing interests: The author(s) declare that they have no competing interests.

Acknowledgements

Funding for this project was supplied to AB by Murdoch University Australian Postgraduate Award and was supported by funding from the Western Australian Government's State NRM Program, and the Department of Parks and Wildlife (DPaW). Thanks to the facilities of the Australian Microscopy & Microanalysis Research Facility at the Centre for Microscopy, Characterisation & Analysis in the University of Western Australia.

Appendix A. Supplementary Data

Supplementary data associated with this article can be found, in the online version, at http://dx.doi.org/10.1016/j.protis.2015.11.002.

References

Andrade LO, Machado CR, Chiari E, Pena SD, Macedo AM (2002) *Trypanosoma cruzi*: role of host genetic background in the differential tissue distribution of parasite clonal populations. Exp Parasitol **100**:269–275

Austen J, Jefferies R, Friend J, Ryan U, Adams P, Reid S (2009) Morphological and molecular characterization of *Trypanosoma copemani* n. sp. (Trypanosomatidae) isolated from Gilbert's potoroo (*Potorous gilbertii*) and quokka (*Setonix brachyurus*). Parasitology **136**:783–792

Bastin P, Rotureau RB (2015) Social motility in African trypanosomes: fact or model? Trends Parasitol **31**:2–37

Botero A, Thompson CK, Peacock CS, Clode PL, Nicholls PK, Wayne AF, Lymbery AJ, Thompson R (2013) Trypanosomes genetic diversity, polyparasitism and the population decline of the critically endangered Australian marsupial, the brush tailed bettong or woylie (*Bettongia penicillata*). Int J Parasitol: Parasites and Wildlife **2**:77–89

Carreira JCA, Jansen AM, Deane MP, Lenzi HL (1996) Histopathological study of experimental and natural infections by *Trypanosoma cruzi* in *Didelphis marsupialis*. Memórias do Instituto Oswaldo Cruz **91**:609–618

D'Alessandro P, Behr M (1991) *Trypanosoma lewisi* and its Relatives. In Krerer J, Baker JR (eds) Parasitic Protozoa. Academic Press, New York, pp 225–263

De Souza W, De Carvalho TMU, Barrias ES (2010) Review on *Trypanosoma cruzi*: host cell interaction. Int J Cell Biol **2010**:295394

Edwards H, Thompson RCA, Koh WH, Clode PL (2011) Labeling surface epitopes to identify *Cryptosporidium* life stages using a scanning electron microscopy-based immunogold approach. Mol Cellul Probes **26**:21–28

Eger-Mangrich I, de Oliveira M, Grisard EC, De Souza W, Steindel M (2001) Interaction of Trypanosoma rangeli Tejera, 1920 with different cell lines in vitro. Parasitol Res **87**:505–509

Grace TDC, Brozostowski HW (1966) Analysis of the amino acids and sugars in an insect cell culture medium during cell growth. J Insect Physiol **12**:625–633

Harshey RM (2003) Bacterial motility on a surface: many ways to a common goal. Annu Rev Microbiol **57**:249–273

Hoare CA (1972) The Trypanosomes of Mammals. A Zoological Monograph. Blackwell Scientific, Oxford, 749 p

Imhof S, Knüsel S, Gunasekera K, Vu XL, Roditi I (2014) Social motility of African trypanosomes is a property of a distinct life-cycle stage that occurs early in tsetse fly transmission. PLoS Pathogens **10**:e1004493

Lara F, Sant'Anna C, Lemos D, Laranja G, Coelho M, Reis Salles I, Michel A, Oliveira P, Cunha-e-Silva N, Salmon D (2007) Heme requirement and intracellular trafficking in *Trypanosoma cruzi* epimastigotes. Biochem Biophys Res Commun **355**:16–22

Lima L, da Silva FM, Neves L, Attias M, Takata CSA, Campaner M, de Souza W, Hamilton PB, Teixeira MMG (2012) Evolutionary Insights from bat trypanosomes: Morphological, developmental and phylogenetic evidence of a new species, *Trypanosoma* (Schizotrypanum) *erneyi* sp. nov., in African bats closely related to *Trypanosoma* (Schizotrypanum) *cruzi* and allied species. Protist **163**:856–872

Lima L, Espinosa-Álvarez O, Hamilton PB, Neves L, Takata CSA, Campaner M, Attias M, de Souza W, Camargo EP, Teixeira MMG (2013) *Trypanosoma livingstonei*: a new species from African bats supports the bat seeding hypothesis for the *Trypanosoma cruzi* clade. Parasit Vectors **6**:221

Miranda K, Benchimol M, Docampo R, de Souza W (2000) The fine structure of acidocalcisomes in *Trypanosoma cruzi*. Parasitol Res **86**:373–384

Molyneux D (1976) Biology of Trypanosomes of the Subgenus Herpetosoma. In Lumsden WHR, Evans DA (eds) Biology of the Kinetoplastida. Academic Press, London, pp 285–325

Noyes H, Stevens J, Teixeira M, Phelan J, Holz P (1999) A nested PCR for the ssrRNA gene detects *Trypanosoma binneyi* in the platypus and *Trypanosoma* sp. in wombats and kangaroos in Australia. Int J Parasitol **29**:331–339

Oberholzer M, Lopez MA, McLelland BT, Hill KL (2010) Social motility in african trypanosomes. PLoS Pathogens **6**:e1000739

Oliveira MPdC, Cortez M, Maeda FY, Fernandes MC, Haapalainen EF, Yoshida N, Mortara RA (2009) Unique behavior of *Trypanosoma dionisii* interacting with mammalian cells: Invasion, intracellular growth, and nuclear localization. Acta Tropica **110**:65–74

Rodrigues A, Campaner M, Takata C, Dell'Porto A, Milder R, Takeda G, Teixeira M (2003) Brazilian isolates of *Trypanosoma*(Megatrypanum) *theileri*: diagnosis and differentiation of isolates from cattle and water buffalo based on biological characteristics and randomly amplified DNA sequences. Vet Parasitol **116**:185–207

Schneider I (1964) Differentiation of larval *Drosophila* eye antennal discs in vitro. J Exp Zool **156**:91–103

Sudarto M, Tabel H, Hainies D (1990) Immunohistochemical demonstration of *Trypanosoma evansi* in tissues of experimentally infected rats and a naturally infected water buffalo (*Bubalus bubalis*). J Parasitol **76**:162–167

Tanoura K, Yanagi T, de Garcia VM, Kanbara H (1999) *Trypanosoma rangeli* in vitro metacyclogenesis and fate of metacyclic trypomastigotes after infection to mice and fibroblast cultures. J Eukaryot Microbiol **46**:43–48

Thompson CK, Botero A, Wayne AF, Godfrey SS, Lymbery AJ, Thompson R (2013) Morphological polymorphism of *Trypanosoma copemani* and description of the genetically diverse *T. vegrandis* sp. nov. from the critically endangered Australian potoroid, the brush-tailed bettong (*Bettongia penicillata*)(Gray, 1837). Parasit Vectors **6**:121

Tizard I, Gorski J, Sheppard J, Mellors A, Hambrey P (1980) Studies on the generation of biologically active substances by *Trypanosoma theileri* in vitro. Res Vet Sci **28**:178–184

Velicer GJ, Kroos L, Lenski RE (2000) Developmental cheating in the social bacterium *Myxococcus xanthus*. Nature **404**:598–601

Wayne AF, Maxwell MA, Ward CG, Vellios CV, Wilson I, Wayne JC, Williams MR (2013b) Sudden and rapid decline of the abundant marsupial *Bettongia penicillata* in Australia. Oryx **49**:1–11

Wayne AF, Maxwell M, Ward CG, Vellios CV, Ward BG, Liddelow GL, Wilson I, Wayne JC, Williams MR (2013a) Importance of getting the numbers right: quantifying the rapid and substantial decline of an abundant marsupial, *Bettongia penicillata*. Wildlife Res **40**:169–183

Zúñiga C, Paláu M, Penin P, Gamallo C, de Diego J (1997a) *Trypanosoma rangeli*: increase in virulence with inocula of different origins in the experimental infection in mice. Parasitol Res **83**:797–800

Zúñiga C, Palau T, Penin P, Gamallo C, de Diego J (1997b) Characterization of a *Trypanosoma rangeli* strain of Colombian origin. Memórias do Instituto Oswaldo Cruz **92**:523–530